Journal of Organometallic Chemistry, 340 (1988) 203–222
Elsevier Sequoia S.A., Lausanne – Printed in The Netherlands

The mechanism of organometallic migration reactions. A configuration mixing (CM) approach

Alan J. Shusterman*,
Department of Chemistry, Pomona College, Claremont, CA 91711 (U.S.A.)

Idan Tamir and Addy Pross*
Department of Chemistry, Ben Gurion University of the Negev, Beer Sheva, 84105 (Israel)

(Received August 3rd, 1987)

Abstract

The configuration mixing (CM) model is applied to the migratory insertion of carbon monoxide into a transition metal–carbon bond. A qualitative reaction profile for the reaction is constructed using an energy plot of the three electronic configurations, which describe the reactant, the product, and the five-coordinate intermediate. The model provides a simple picture of reactivity trends in these systems, as well as indicating the way in which a mechanistic spectrum, encompassing both step-wise and concerted pathways, is generated. The model analyzes the effect of modifications of the migrating group, the acceptor group, and the entering ligand. Migratory insertion assisted by either prior oxidation or reduction of the starting metal complex is also considered. The conclusions are supported by experimental and computational data.

Introduction

Migratory insertion of carbon monoxide into a metal carbon bond (eq. 1) is one of the most widely studied reactions in organo-transition metal chemistry [1]. It constitutes an important step in a number of homogeneous catalytic transformations, and because of its ability to functionalize CO is of considerable synthetic utility. In addition to the many mechanistic papers that have appeared on this subject, the process has also been the focus of a number of theoretical analyses [2,3]. As a result, many of the features of this reaction are now reasonably well-established.

$$L + R\text{–}M\text{–}CO \rightarrow L\text{–}M\text{–}CO\text{–}R \quad (1)$$

0022-328X/88/$03.50

Despite the extensive literature coverage of these reactions, we believe there is currently no simple model for relating the many diverse observations that have been made. In this paper we utilize the configuration mixing (CM) model [4] which has been applied over the years to a number of problems in physical and mechanistic organic chemistry, to address this particular question. By building up a simple qualitative description of a reaction profile for the CO insertion reaction we hope to demonstrate how many features of these reactions, including some that remain controversial, may be understood.

In the course of this analysis, we hope to demonstrate that the CM model can serve as a conceptual framework for "thinking" about organometallic reactivity. By applying the model to the migratory insertion reaction, we can show how many general aspects of chemical reactivity may be appreciated in qualitative terms. It is our belief that the enormous strides made over recent years in computational procedures have to some extent overshadowed the search for those key elements that determine the outcome of a particular calculation. In our view, the CM model helps overcome this problem by identifying the principal factors governing barrier heights, i.e., reactivity, and the nature of the reaction profile.

Theory

The configuration mixing (CM) model provides insight into problems of reactivity and reaction mechanism by qualitatively building up a simple description of a reaction profile from configuration building blocks [4]. The key configurations that go into the description of any reaction profile are the so-called reactant and product configurations, R and P respectively. The reactant and product configurations are so named because the valence electrons are arranged in a way that correspond to the electron distribution present in the reactant and product molecules. Additional configurations, I, whose electrons are arranged so that they describe potential intermediates along the reaction pathway, may also be required in order to describe the reaction profile more completely. These configurations may be indicated on the basis of experimental information regarding the reaction mechanism or by calculations that reveal the electron distribution at different points along the reaction coordinate.

The R and P configurations, while implicitly describing all of the electrons in the reacting system, explicitly treat only those electrons involved in the reaction, i.e., electrons associated with bonds that are broken or formed during the reaction. The remaining electrons can be viewed as a "core" that is not greatly affected by the reaction and which does not contribute significantly to the energetic changes that occur. Since the two electron pairs that rearrange during the CO insertion reaction (eq. 1) are those associated with the M–R bond and the lone pair of the incoming ligand, L, the various configurations may be obtained by rearranging these four key electrons. Our theoretical arguments, which apply not just to CO insertion reactions, but also to insertions by any other π acceptor ligand, will be developed at present without reference to a particular molecular system.

A priori, configurations may be described in either valence-bond (VB) or molecular orbital (MO) terminology. Since the VB approach can describe the configurations using simple Lewis structures, bonding changes that occur can be depicted in a simple fashion. However, energy differences between configurations and problems

of symmetry are more readily treated using MO concepts. Consequently, the VB approach will form the basis of this paper while MO arguments will be introduced to clarify aspects not apparent in the VB treatment.

VB Configurations

The classical VB treatment employed here views chemical bonds as the sharing of electrons by two atoms [5]. In a polyatomic system we define each bond by specifying a particular spin-pairing arrangement of the electrons. Different electronic configurations are obtained by either changing the spin-pairing arrangements or by transfer of an electron(s) from one atom to another. The true wavefunction, which can always be expressed as a linear combination of these different configurations, as is qualitatively done using resonance structures, will in many cases be dominated by a single electronic configuration. In these cases it will be a good approximation to view the wavefunction solely in terms of the properties of the dominant configuration.

The reactant configuration, *R*, for the reaction of eq. 1, is illustrated in Table 1 and is just that electronic configuration which provides a satisfactory description of the reactant state, i.e., the metal alkyl carbonyl complex and the free ligand. Note that the four key valence electrons are shown explicitly; the M–R bond is depicted by the Heitler–London wavefunction form, R↑. .↓M, and the ligand lone pair by L:.

Table 1

Electron configurations (VB and MO) for reactant, *R*, intermediate, *I*, and product, *P*, configurations

Configuration	Model	Reactant geometry	Intermediate geometry	Product geometry
R	VB	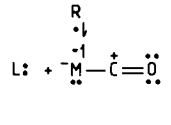	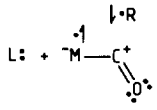	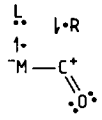
I	VB	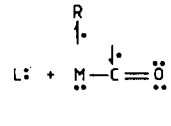	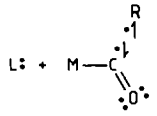	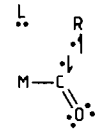
P	VB	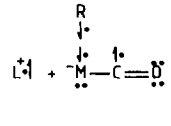	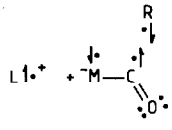	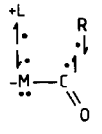
R	MO	$(\sigma_{MR})^2(n_L)^2$		
I	MO	$(\sigma_{MR})^1(\pi^*_{MCO})^1(n_L)^2$		
P	MO	$^3((\sigma_{MR})^1(\sigma^*_{MR})^1)^3((n_L)^1(\pi^*_{MCO})^1)$		

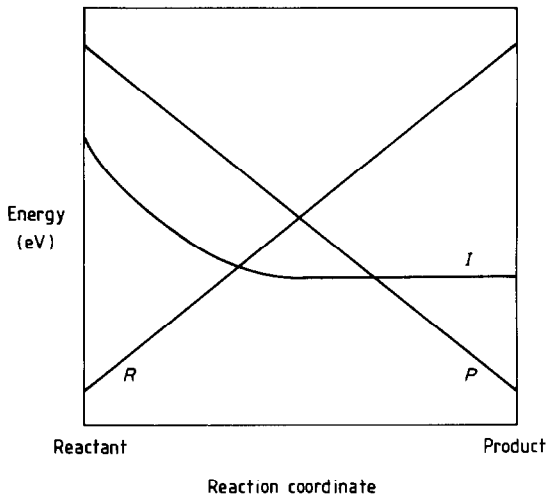

Fig. 1. Schematic energy diagram for R, I, and P configurations (see Table 1) as a function of the nuclear reaction coordinate for the migratory insertion of CO into a metal–carbon bond (eq. 1).

The energy of R is highly dependent on nuclear position. In the *reactant* geometry, indicated in Table 1, R is low in energy; it is a ground configuration. However, its energy increases along the reaction coordinate (migration of R, approach of L), because this involves both stretching of the M–R bond, and introduction of a repulsive 3-electron interaction between L: and M. This point becomes clear by examining configuration R in the *product* geometry (Table 1). Clearly, in this geometry R is a high energy entity since the electronic distribution in R does not facilitate either an M–L or an R–C bond, both of which exist in the product. The energy change of R along the reaction coordinate is shown schematically in Fig. 1. As discussed above, R must increase in energy along the reaction coordinate.

The VB product configuration, P, has its electrons arranged so that it can provide a good electronic description of the reaction *product*, the acyl complex L–M(CO)R (Table 1, product geometry). Thus, the four electrons in P are organized into an L↑. .↓M pair representing the newly formed L–M bond, and a C↑. .↓R pair representing the new C–R bond. In the reactant geometry, P is high in energy since neither the M–L nor C–R bonds are actually formed as yet (Table 1, reactant geometry), i.e., in the reactant geometry P is an excited configuration. At the product geometry, however, P is the ground configuration and the energy of P drops along the reaction coordinate accordingly (Fig. 1).

In this particular reaction, there is experimental evidence for a coordinately unsaturated intermediate, I, containing an acyl ligand but no M–L bond. Since neither of the two configurations presented thus far provides a good description of this intermediate, we now introduce a third configuration, I. At the intermediate geometry I is a ground configuration, but at the reactant and product geometries it will be an excited configuration (Table 1). The four electrons in configuration I are organized into a lone pair on L and a bonding pair, C↑. .↓R, describing the new carbon–carbon bond.

M–CO–R
(I)

Since configuration I has features in common with both the reactants (lone pair on L) and the product (C–R bond) its energy is a less sensitive function of the reaction coordinate than are the energies of configurations R and P. The energy of I, as a function of the reaction coordinate, is shown schematically in Fig. 1. Note that the energy curve for I, while flat compared to those of R and P, does drop along the reaction coordinate. This is because migration of R facilitates coupling of the spin-paired electrons on R and C into an R–C bond. At the reactant and product geometries, I is an excited configuration, and can be obtained from R and P by just a single electron excitation. At the reactant geometry, formation of I involves the transfer of an electron from M to C, while at the product geometry I constitutes an excited configuration of the M–L bond, describing it as L: M in place of L↑. .↓M (Table 1).

MO Configurations

The preceding VB analysis makes it easy to visualize the bonding changes that occur during the migration reaction in eq. 1 by expressing the wavefunction in terms of three configurations R, P, and I. It is possible to generate similar MO configurations by rearranging the four key electrons among the various molecular orbitals of the reactants. This approach allows us to express the energy differences between the different configurations, to a first approximation, in terms of the properties of these orbitals. The important orbitals in this reaction are the non-bonding orbital on L, n_L, the M–R bonding orbital, σ_{MR}, and the vacant orbital on the migration terminus, $\pi^{\star}_{MCO}$. Different electron occupations of these orbitals, as well as different spin-pairings, are used to form the required configurations. Despite the use of orbitals that are defined only at the reactant geometry, consideration of just three MO configurations is sufficient to grasp the key energetic features of the entire reaction profile. This will enable us to subsequently predict substituent effects on reactivity.

The reactant configuration R, consists of doubly occupied orbitals, n_L and σ_{MR}. The change that converts R to I, according to the VB terminology, is an electron shift from the metal atom, M, to the carbonyl carbon atom. From the MO point of view, the electron originates from the σ_{MR} orbital, and is shifted into a $\pi^{\star}_{MCO}$ orbital, concentrated on the carbonyl carbon atom. Thus, in MO language, R to I excitation is brought about by a $\sigma_{MR} \rightarrow \pi^{\star}_{MCO}$ electron shift, and the double excitation required to convert R to P is $\sigma_{MR} \rightarrow \sigma^{\star 3}_{MR}$ and $n_L \rightarrow \pi^{\star 3}_{MCO}$; the double triplet excitation of the product configuration allows it to retain overall singlet character. The MO configurations at the reactant geometry are listed in Table 1 (reactant geometry) as excitations from configuration R so that the basis for assigning the relative energies of R, P, and I, namely, $P > I > R$, at this geometry now become evident (Fig. 1).

In the discussion that follows we shall employ both VB and MO configurations to elaborate the reaction profile. It should be kept in mind that even though the three VB configurations share certain characteristics with the three MO configurations, the two terminologies are not identical. For example, the R VB configuration and the R MO configuration, which are both ground configurations at the reactant geometry, yield different electronic energies and distributions. In general, we will refer to the VB configurations to answer questions concerning bonding. Substituent effects and reactivity trends, on the other hand, will be explained mainly in terms of MO configurations and orbital properties.

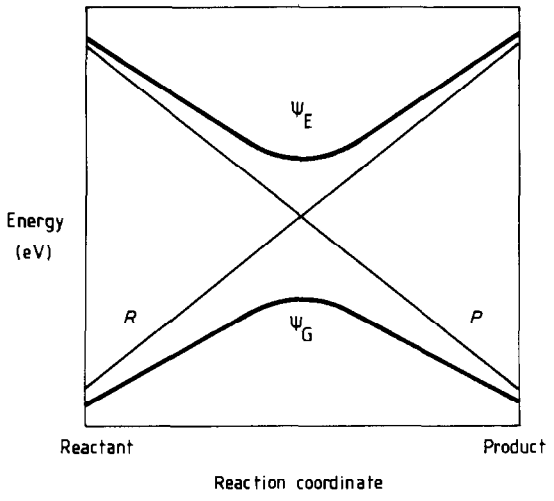

Fig. 2. Schematic energy diagram that illustrates the mixing of R and P configurations leading to an avoided crossing and generation of a ground state surface, ψ_G, and an excited state surface, ψ_E (bold lines).

Configuration Mixing (CM)

Having described a set of three configurations, we can now construct a reaction profile using a linear combination of these configurations. The simplest possible description of the reaction profile, which connects the reactant and product ground states, is obtained from a linear combination of R and P. These can combine in either an in-phase manner to generate a ground state surface, Ψ_G, or in an out-of-phase manner to generate an excited state surface, Ψ_E, as indicated in eqs. 2 and 3, where a and b are coefficients. The mixing process is shown in Fig. 2. The configuration crossing thus leads to a *state* avoided crossing (bold curves, Fig. 2). The extent to which the crossing is avoided depends on the magnitude of the overlap of R and P. Further away from the configuration crossing point, the contribution made by each configuration to the ground state wavefunction is determined by the energy of that configuration, in addition to its overlap with the other configurations. In this paper we will only discuss the ground state surface, ψ_G, and its component configurations.

$$\Psi_G = aR + bP \tag{2}$$

$$\Psi_E = -bR + aP \tag{3}$$

Mixing of I into Ψ_G, as defined by eq. 4, can lead to an improved description of the ground state wavefunction. More importantly, variations in the energy of I will be shown to control the mechanism of the CO insertion reaction.

$$\Psi_G = aR + bP + cI \tag{4}$$

Discussion

A. Two-step mechanism – unassisted migration

Up to this point our presentation of the CO insertion reaction has been general and can be adapted to a wide variety of molecular systems. In order to demonstrate

how the CM model can be applied to a particular reaction we will consider the process shown in eq. 5, namely, the conversion of methyl(pentacarbonyl)manganese-(I) (**2**) to acetyl(tetracarbonyl)(ligand)manganese(I) (**3**). This system has been carefully studied from both an experimental and theoretical point of view and provides a good basis for demonstrating the CM analysis.

$$\underset{(\mathbf{2})}{(CO)_5Mn{-}CH_3} + L: \rightarrow \underset{(\mathbf{3})}{(CO)_4(L)Mn{-}COCH_3} \tag{5}$$

The CO insertion reaction shown in eq. 5 is actually an alkyl migration reaction in which the methyl group migrates to a *cis* CO ligand; the entering ligand, L, then occupies the position originally taken by the methyl group [6]. The reaction is reversible, and the kinetics of both the forward and reverse reactions have been investigated under a diverse set of experimental conditions [7]. Most discussions of the reaction have made use of the two-step mechanism shown in eqs. 6 and 7, i.e., a migration of the methyl group to give a coordinately unsaturated intermediate, followed by the formation of a new manganese–ligand bond. According to this mechanism, the methyl migration is a unimolecular rearrangement, unassisted by any external ligand.

$$\underset{(\mathbf{2})}{(CO)_5Mn{-}CH_3} \underset{k_{-1}}{\overset{k_1}{\rightleftarrows}} \underset{(\mathbf{4})}{(CO)_4Mn{-}COCH_3} \tag{6}$$

$$\underset{(\mathbf{4})}{(CO)_4Mn{-}COCH_3} + L \xrightarrow{k_2} \underset{(\mathbf{3})}{(CO)_4(L)Mn{-}COCH_3} \tag{7}$$

Several kinetic investigations of the CO insertion reaction undergone by manganese complex **2** have produced the rate law given in eq. 8 [7b,c,e]. The two-step mechanism (eqs. 6 and 7) is consistent with this rate law provided the intermediate is at steady-state. Reaction conditions yielding simpler rate expressions have also been found, but these examples have been generally regarded as limiting cases of the same stepwise process; a rate-limiting first step, i.e., $k_2[L] \gg k_{-1} > k_1$, results in an apparent first-order reaction with $k_{obsd} = k_1$, while an initial pre-equilibrium followed by a rate-limiting second step, $k_{-1} \gg k_2[L]$, yields a second-order rate expression where $k_{obsd} = (k_1 k_2 / k_{-1})[L]$. Additional observations consistent with this mechanism include: (a) the first-order rate constant k_1 is insensitive to the entering ligand [1], (b) intermediate **4** has been synthesized independently in inert matrices at low temperature [8], and (c) calculations have indicated that **4** corresponds to a local minimum on the potential energy surface [2a,3b].

$$\frac{d[MnCH_3]}{dt} = \frac{k_1 k_2 [L]}{(k_{-1} + k_2[L])} \times [MnCH_3] \tag{8}$$

Application of the CM model

Construction of a reaction profile for this mechanism using the CM model proceeds from a consideration of the reaction coordinate; this coordinate must contain three local minima, corresponding to the reactants, product, and intermediate: species **2** + L, **3**, and **4** + L. These minima are well described by configurations *R*, *P*, and *I*, respectively, leading to the energy diagram shown in Fig. 3. From

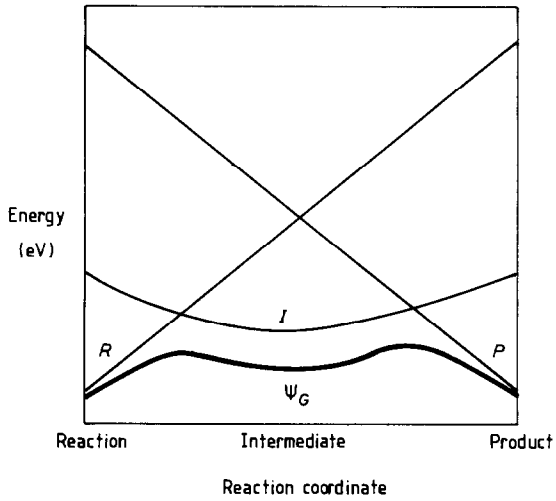

Fig. 3. Schematic energy diagram for a two step process for the reaction of eq. 1 (bold curve) that is generated from R and P and a low-lying I configuration.

this diagram we can see that two avoided crossings are produced, each corresponding to a single electron shift. The first transition state is an admixture of configurations R and I and involves a $\sigma_{MR} \rightarrow \pi^{\star}_{MCO}$ shift. The second transition state is composed of configurations I and P and involves a $n_L \rightarrow d_M$ shift. The actual reaction profile, brought about by the mixing of R, P, and I, is described by the bold curve (Fig. 3).

Determining the actual barrier heights, or even the relative height of the two barriers, requires a detailed knowledge of orbital energies and overlaps that is outside the framework of the our qualitative model. However, the CM model, by clearly defining the electron rearrangement associated with each barrier, allows one to identify the factors that shape each barrier. In particular, we shall show how the character of the migrating group, the acceptor group, and the incoming ligand influences the rate of each reaction step.

The influence of the migrating group, R. The influence of the migrating group is felt mainly during the migration step (eq. 6). Ignoring steric effects, we find that according to the model, the barrier height for this step depends on the energetic separation of the σ_{MnR} and $\pi^{\star}_{MnCO}$ orbitals. A large energy gap will lead to a large activation barrier. Photoelectron spectra of $(CO)_5Mn-R$ complexes show that the σ orbital energy is a sensitive function of the electronegativity of the alkyl ligand [9]. The size of the barrier, then, is expected to be controlled by the electronegativity of the alkyl group, since this controls the energy of the σ orbital.

The reaction profiles for the migration step for two different alkyl complexes are given in Fig. 4. The barrier to the migration process, $E_1^{\neq}$, is attributed to the avoided crossing (deleted for clarity) of the R and I configurations. If the alkyl group is now replaced by a *less* electronegative alkyl group this has the effect of *decreasing* the $\sigma \rightarrow \pi^{\star}$ transition. As a consequence the I configuration is stabilized with respect to R (indicated by I' and dotted line of Fig. 4), and a *lower* migration barrier results ($E_1^{\neq} > E_2^{\neq}$). The above prediction is borne out experimentally. It has

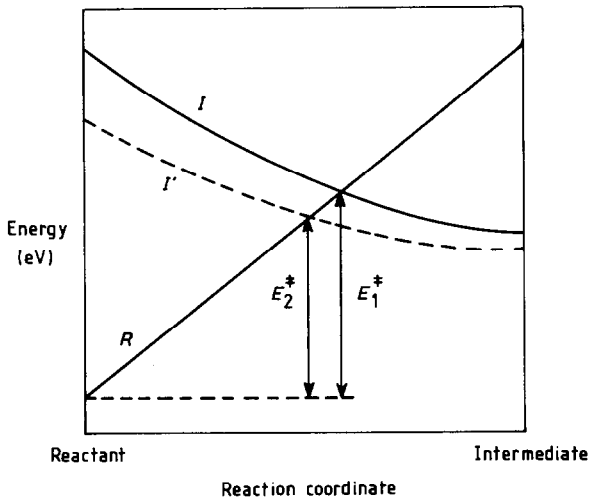

Fig. 4. Schematic energy diagram illustrating the barrier, E_1^*, to alkyl migration for a given alkyl group, R, generated from *R* and *I* configurations. A reduced barrier, E_2^*, is obtained when the alkyl group is made less electronegative since *I'* (dotted line) is now stabilized relative to *I*.

been reported that as the electronegativity of the alkyl ligand increases, its migratory ability decreases. The carbonylation rate of different alkyl manganese complexes decreases in the order n-$C_3H_7 > C_2H_5 > C_6H_5 > CH_3 \gg CH_2C_6H_5$ or CF_3 (eq. 5, L = CO) [11]. Another trend that has been observed is $CH_3 > CH_2F \gg CF_3$ (eq. 5, $L = I^-$) [7f]. The migratory abilities of various *para*-substituted benzyl complexes (L = CNR) can also be correlated with the electronegativity of the benzyl group. The reaction shown in eq. 9 did not occur when $X = NO_2$, while with more electron-donating substituents the rate decreased in the order $X = CH_3 > H > Cl$ [12]. Since the same steric effects occur in each member of this series, the failure of the nitro-substituted material to react must be attributed to the strong electron-withdrawing influence of the nitro group, which is communicated to the carbon–metal bond. EHMO calculations also reveal this correlation of alkyl group electronegativity and migration rate [2a].

$$(CO)_5Mn\text{–}CH_2C_6H_4\text{-}p\text{-}X + R\text{–}N{\equiv}C: \rightarrow (RNC)(CO)_4Mn\text{–}COCH_2C_6H_4\text{-}p\text{-}X \quad (9)$$

Unfortunately, it is not easy to compare alkyl ligands with other potential migrating ligands, such as hydride, silyl, or aryl groups. Even though the same electron rearrangement is required in each case, the variation in ligand properties as represented by orbital size, availability of π-type orbitals, etc., makes direct comparison of different ligands difficult. For example, $(CO)_5Mn\text{–}SiR_3$ ($R = CH_3$ or C_6H_5) which contains a very electropositive silyl group, does not undergo CO insertion [13].

The influence of the acceptor group. The acceptor group acting as the migration terminus can affect the rate of the migration step (eq. 6) by governing the energy of the reacting $\pi^\star$ orbital. Generally speaking, stronger π-acceptor ligands with a lower energy $\pi^\star$ orbital should be able to stabilize configuration *I* relative to configuration *R* leading to a more rapid alkyl migration (Fig. 4). This stabilization

occurs because, as was just discussed, $R \rightarrow I$ conversion involves a $\sigma \rightarrow \pi^\star$ electron shift.

This prediction is borne out by the observation that Lewis acids can markedly accelerate alkyl migration reactions (eq. 10) [14]. It appears that the acid coordinates to a carbonyl oxygen atom, thereby activating that group for the migration reaction. In orbital terminology, the formation of the oxygen–acid bond lowers the energy of the carbonyl $\pi^\star$ orbital, making the ligand a better π-acceptor (withdrawal of electron density from any group tends to lower the energies of both bonding and antibonding orbitals). Lewis acid coordination has an additional effect beyond that of stabilizing the $\pi^\star$ orbital; it also allows the formation of a strong oxygen–acid bond. Consideration of the three configurations suggests that *I* and *P* can form a stronger oxygen–Lewis acid bond than can the *R* configuration, which will also have the effect of enhancing the reaction rate. Thus, in general we can assert that substituent effects which either raise the energy of σ_{MnR} or lower the energy of $\pi^\star_{MnCO}$ will enhance the migration process.

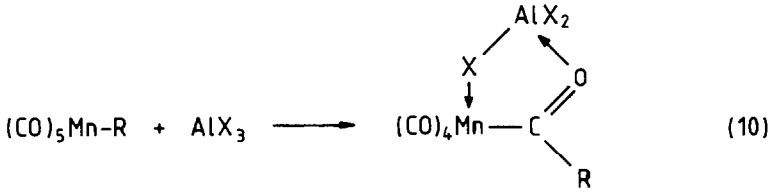

(10)

In view of the simplicity of this analysis, it is somewhat surprising that confusion still persists regarding the mechanism of Lewis acid catalysis. Some have argued that coordination of the carbonyl ligand to the acid should actually *deactivate* the molecule since electron transfer from the metal to the carbonyl ligand is increased [2b]. In fact, formation of an acid–oxygen bond should result in an overall decrease in electron density on the carbonyl carbon, i.e., the carbonyl is activated, since the increase in metal-to-carbon π-donation can only partially compensate for the decrease in oxygen-to-carbon π-donation.

Comparison of the relative reactivity of different π-acceptor ligands as migration termini is also possible. Since π-acceptor ability decreases in the order $NO^+ > CO > CNR$ the CM model predicts that the rate of alkyl migration to these different ligands will decrease in the same order. There is no systematic experimental evidence that refutes or confirms this prediction unambiguously. The reactivity order towards insertion is usually given as $CNR > CO > NO^+$, the exact opposite of the CM model's prediction. The basis for this ordering comes from two different types of observations. First, many examples of carbonyl and isonitrile insertions have been reported, while nitrosyl insertions have remained rare [15]. Second, ligands such as hydrogen, which normally resist carbonyl insertion, do undergo isonitrile insertion [16]. An interesting counter-example is provided by complexes of the type *cis*-$(CO)_4(CNR)Mn–R$. Treatment of these complexes with phosphines gives only the products of carbonyl insertion [12].

EHMO calculations have been applied to the case of methyl migration in the complex *cis*-$(CO)_4(L)Mn–CH_3$ ($L = NO^+$, CO, CNR) [2a]. In this case, the calculated reactivity order was given as $CO \geq NO^+ > CNR$. These calculations found that one reason for the lower reactivity of nitrosyl, relative to carbonyl, is due to the loss of metal–nitrosyl π-bonding in the π system perpendicular to the migration

plane, subsequent to the generation of the nitroso ligand. This energy change does not involve the reacting electrons identified by the CM model and points out the fact that in some cases, too great a perturbation of the reacting system will result in effects that are unrelated to the electron shifts needed to accomplish the reaction.

Influence of the entering ligand. The avoided crossing that occurs between the *I* and *P* configurations is somewhat different from the one linking *R* and *I*. Conversion of *R* to *I* requires the rearrangement of one bonding pair into another, whereas *I* to *P* conversion involves the change of a lone pair, n_L, into a bonding pair. Consequently, it may seem that no activation energy is required for the $n_L \rightarrow d_M$ electron shift, i.e., it may appear that as the L–Mn distance decreases the energy of *I* will remain flat or maybe even decrease. In fact, several factors can operate to cause an *increase* in the energy of *I* during ligand–metal bond formation resulting in an energy barrier. Among these are: (a) changes in the geometry of **4**, (b) steric repulsion between L and **4**, and (c) changes in the solvation of L and **4** along the reaction coordinate.

Different studies have suggested various structures for intermediate **4**; for example, matrix-isolated **4** appears to have a pseudo-trigonal bipyramidal structure [8]. On the other hand, labelling studies indicate that **4**, generated during the insertion reaction (eq. 5, $L = P(OCH_2)_3CCH_3$), actually possesses a pseudo-square-pyramidal geometry [6b]. These contrasting results are perhaps due to the different environments of **4** in each study: an inert matrix versus a potentially coordinating solvent. Theoretical calculations on **4** have appeared, supporting both the trigonal-bipyramidal [3b] and square-pyramidal [2a] alternatives. Since *I* is the ground configuration of intermediate **4**, any structural rearrangement of **4** required for the formation of **3** will be accompanied by an increase in the energy of *I* as the avoided crossing is approached.

The analysis of solvent–intermediate interactions is complicated by the potential formation of an acyl complex containing a solvent molecule as a donor ligand, i.e., $(CO)_4$(solvent)Mn–$COCH_3$. While no such solvent complexes have been isolated from this manganese system, there is spectroscopic evidence for their formation in this system and others [7a,17]. The intermediacy of a metastable solvent complex in the alkyl migration reaction means that the formation of the final product, **3**, will require the cleavage of a manganese–solvent bond, a process that might involve a relatively large barrier. This analysis, derived from the properties expected for intermediate **4**, predicts that the overall reaction rate should decrease upon replacing a poor donor solvent with a better donor solvent. In fact, just the opposite is true; the CO insertion reaction is accelerated by a solvent in proportion to that solvent's donating ability [7a,c,d,e,18b]. Thus, solvent assistance of the migration reaction cannot be reconciled with the two-step mechanism of eqs. 6 and 7, or with any other mechanism that postulates an unassisted migration. We shall return to the question of the solvent-assistance when we discuss the one-step ligand-assisted migration mechanism.

Comparison of the CM model with theoretical calculations. It is interesting to compare the qualitative description of the reaction profile provided by the CM model with the results of theoretical calculations. Two sets of extended Hückel MO (EHMO) calculations have been reported for the reaction of eq. 5, including a detailed account of the potential energy surface for the alkyl migration given in eq. 6 [2]. The conclusion of both investigations was that a four-electron destabilizing

interaction between the migrating methyl group and the σ_{MnC} pair connecting the carbonyl ligand to the metal was responsible for the calculated barrier. Another calculation, one of the CNDO type, analyzed the reactivity of the manganese complex entirely in terms of charge densities and bond indices present in the starting metal alkyl complex [3a].

The picture that emerges from the CM model is quite different. According to the CM model, these energy barriers result from the energy required to rearrange the four *reacting* electrons, and this can be understood only in terms of the configurational changes that take place along the reaction coordinate. Yet despite the different interpretations of the factors governing barrier formation it is possible to show that these calculations do, in fact, show many features consistent with the predictions of the CM model. For example, examination of the EHMO orbital diagram for the tetracarbonyl acyl complex, **4**, reveals that the carbon–carbon bond orbital, which replaces the σ_{Mn-CH_3} orbital during the alkyl migration, contains a significant contribution from the carbonyl $\pi^\star$ orbital, consistent with a $\sigma_{MnR} \rightarrow \pi^\star_{MnCO}$ electron shift. The energy profile of this orbital parallels the calculated rise and fall in total energy, suggesting that the changes that occur in this orbital, i.e., the mixing in of the $\pi^\star$ orbital, are the same ones responsible for the calculated barrier [19]. The CNDO calculations of Ruiz et al., also reinforce our description [3b]. They report changes in bond orders for the entire reaction coordinate allowing comparison with bond orders predicted by the VB-CM model. Their calculations show that in the transition state region the decrease in $Mn–CH_3$ bond order is compensated by a matching increase in $C–CH_3$ bond order. At the same time, a substantial decrease is observed in the C–O bond order of the incipient acyl ligand, all of which is consistent with the predicted crossover of configuration *R* into configuration *I*, and a transition state described by a linear combination of configurations *R* and *I*. The above considerations indicate that the EHMO and CNDO results actually confirm the basic features of the CM model, as well as suggest ways in which the CM analysis can aid in the interpretation of theoretical calculations.

B. One-step mechanism – ligand-assisted CO insertion

Migratory insertion of CO can also occur via a concerted mechanism in which the migration of the alkyl group is assisted by the new ligand, L (eq. 10); this results in simultaneous formation of new carbon–carbon and metal–ligand bonds. Solvent-assisted migration can be explained by the same mechanism by replacing L in eq. 10 with a solvent molecule. This reaction produces an unstable solvated acyl complex, $(CO)_4$(solvent)$Mn–COCH_3$, that is converted into **3** upon reaction with L. The reaction profile for ligand or solvent-assisted CO insertion is readily constructed using the same three electronic configurations we had employed in our treatment of the stepwise mechanism for unassisted CO insertion (eqs. 6 and 7). Since the ligand-assisted migration has not been widely discussed, we shall first review some of the key experimental and theoretical data supporting this mechanism.

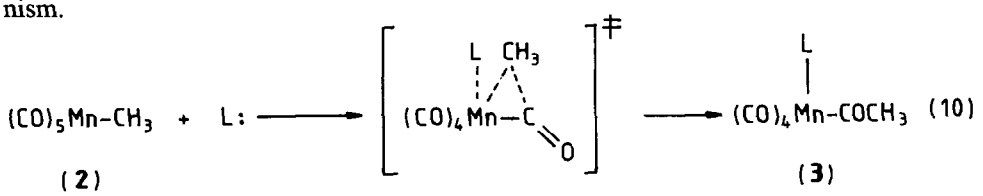

The experimental evidence favoring the operation of a concerted mechanism for CO insertion comes from kinetic studies involving different ligands, and from the observation and characterization of solvent effects in these reactions. The best case for a ligand-assisted CO insertion is provided by the reaction of iodide with $(CO)_5Mn–CH_2F$ to give the anionic acyl complex, $[(CO)_4(I)Mn–COCH_2F]^-$ [7f]. The reaction follows a second-order rate law, similar to eq. 11, consistent with a one-step bimolecular process. An alternative interpretation of the rate law, namely, an unassisted migration followed by rate-limiting trapping of an unsaturated acyl complex (eq. 8, $k_{-1} \gg k_2[L]$), is precluded by the extremely high reactivity of iodide, and by the adherence of the reaction to second-order kinetics over a wide range of iodide concentrations.

$$-\frac{d[MnCH_3]}{dt} = k_{obsd}[L][MnCH_3] \tag{11}$$

Ligand-assisted CO insertion may be important for other less reactive ligands as well. Cyclohexylamine [7c], in hexane and mesitylene, $P(OCH_2)CCH_3$ [7d], in benzene and chloroform, and dimethylacetylenedicarboxylate (dmad) [7e], in benzene and dichloromethane, all appear to react with **2** by means of a concerted mechanism; in each case, the reaction obeys either a pure second-order rate law (eq. 11), or a rate-law containing independent first and second-order terms (eq. 12). The use of a more nucleophilic solvent in these systems invariably results in a change in mechanism characterized by the appearance of either first-order or saturation kinetics (eq. 8), and a marked acceleration of the insertion reaction, i.e., solvent-assisted insertion prevails. Thus, the ligand and solvent appear to compete for **2**, so that the more effective nucleophile induces the CO insertion and then occupies a coordination site in the initial product.

$$-\frac{d[MnCH_3]}{dt} = (k_1 + k_3[L])[MnCH_3] \tag{12}$$

Direct evidence in favor of a nucleophilic role for the solvent has been obtained from studies that utilized a series of sterically encumbered tetrahydrofuran derivatives as the solvent. The reaction of phosphines with $cp(CO)_3Mo–CH_3$ [18a], and with $(CO)_5Mn–CH_2C_6H_5$ [18b], was "catalyzed" most effectively by tetrahydrofuran and least effectively by 2,5-dimethyl-tetrahydrofuran. In addition, the first-order rate constant for migration, k_1, showed a first-order dependence on the concentration of the nucleophilic solvent [18a]. This unequivocal demonstration of a nucleophilic pathway for solvent-assistance, and the change in mechanism to a ligand-assisted migration, upon use of a non-coordinating solvent, as described above, suggest that the ligand and solvent-assisted mechanisms are general. In fact, the independence of k_1 of the entering ligand, cited above in support of the stepwise mechanism for CO insertion, may be due to a similar solvent-assisted reaction operating with each ligand.

Theoretical calculations have also established the credibility of a ligand-assisted CO insertion mechanism. CNDO calculations of the energy surface for methyl migration, both in the absence (eq. 6) and presence of CO (eq. 10, L = CO), revealed that the activation energy for the migation reaction was lower in the presence of CO at every point along the reaction coordinate [3b]. This result had been regarded with some suspicion in the original report since the bonding interaction between the

entering CO ligand and the metal, as measured by the metal–carbon bond order, remained weak until the final stages of the reaction. But, as we shall demonstrate, ligand-assistance of this sort is indeed consistent with the CM model of the reaction profile. Thus, the CNDO calculations supporting a concerted CO insertion should be accepted at face value.

Application of the CM model

Since the concerted mechanism for migratory insertion of CO does not employ any reaction intermediates, CM analysis of the reaction profile can be most simply described by the avoided crossing of just two configurations, *R* and *P* (Fig. 2). The transition state, then, results from simultaneous formation of the new metal–ligand and carbon–carbon bonds. However, a superior description of the reaction profile is obtained by incorporation of configuration *I*. This is depicted in Fig. 5. In contrast to the two-step pathway (Fig. 3), the influence of *I* is smaller since its energy is now higher, a concerted process results. The transition state for the concerted process becomes a linear combination of *R*, *I*, and *P*, i.e., the wavefunction in eq. 4 with *a*, *b*, and *c* of comparable magnitude. This mixing of *I* character into the transition state causes the carbon–carbon bond to develop to a greater extent than the incipient metal–ligand bond. Computational support for this idea comes from the CNDO calculation of a low manganese–carbon bond order between the metal and the external CO ligand until late in the reaction.

We can see that the primary difference between the step-wise process (Fig. 3) and concerted process (Fig. 5) lies in the relative energy of the *I* configuration. In the latter diagram, the energy of *I* is sufficiently high, and the different avoided crossings are close enough together on the reaction coordinate, so as to prevent formation of an acyl intermediate, such as **4**. Thus, the mechanistic spectrum relating step-wise to concerted reaction pathways may be simply understood in terms of the changes in energy of the *I* configuration.

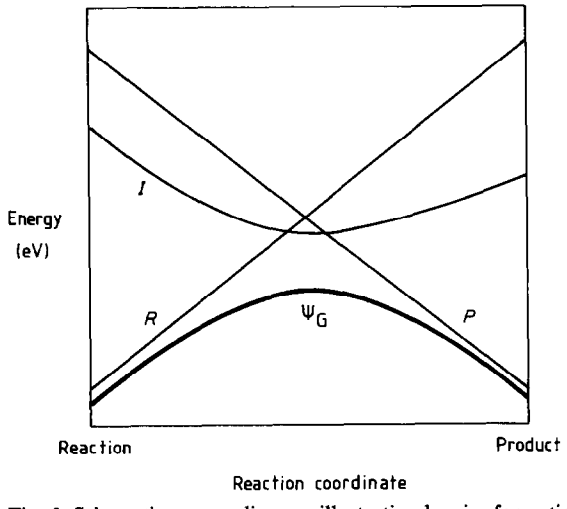

Fig. 5. Schematic energy diagram illustrating barrier formation (bold curve) for the concerted ligand-assisted migratory insertion reaction, using *R*, *I*, and *P* configurations.

Another significant aspect of the reaction profile for the concerted process is that it does not violate the 18-electron rule, despite a formally seven-coordinate metal species in the transition state. *R* and *P* are both 18-electron configurations, while *I* is a 16-electron configuration. *Thus, no linear combination of these three configurations can generate a wavefunction with more than 18-valence electrons on the metal atom.* This contradicts the general notion that any apparent increase in the coordination number of a central atom must increase the number of valence electrons on that atom. Similarly, an associative ligand substitution mechanism for a coordinately saturated metal complex, which appears to require an increase in the metal's coordination number, can be analyzed using only 18-electron configurations.

The similarity of the CM diagrams for the stepwise and concerted insertions facilitates our analysis of the reactivity trends for the latter mechanism. Namely, the three reactivity predictions established for the stepwise process will also apply to the concerted process, except that the reactivity changes must now affect the entire barrier to insertion. Thus, a concerted migratory insertion will be facilitated by a less electronegative migrating group, a better acceptor ligand in the migration terminus, and by a more nucleophilic entering ligand.

One point driven home by the CM model of the concerted insertion, is that reactant and product electron configurations alone, do not accurately describe reaction profiles for reactions requiring a double electron excitation. In these cases, a configuration corresponding to a single electron excitation must be included in the wavefunction. This is, in fact, true for other processes such as elimination [4a] and cycloaddition [4e,f] reactions, and is consistent with the view recently expressed by one of us that much of organic reactivity may be understood on the basis of the energetics of a single electron shift [4f]. In the case of a ligand-assisted migration reaction, mixing in the third configuration, *I*, related to both *R* and *P* by a single electron shift, lowers the energy of the transition state and imparts its own electronic character, i.e., it delays the formation of the metal–ligand bond. This implies that calculations designed to test reaction paths for the participation of an external ligand cannot safely rely on such parameters as bond orders and orbital overlap as the sole criteria for that participation. Rather, a conclusive test must include a calculation of the total energy of the system with and without the external ligand.

C. Electron transfer-assisted migratory insertion

It has been reported recently that one-electron oxidation and reduction of an 18-electron metal alkyl carbonyl complex can induce rearrangement to an odd-electron metal acyl complex [20,21]. In certain cases, migratory insertion of CO is promoted kinetically by the prior redox reaction; we shall term such reactions "electron transfer-assisted." As yet, no satisfactory theoretical explanation of these results has appeared, either qualitative or quantitative.

Electron transfer-assisted migration reactions can be treated in a straightforward manner with the CM model. The necessary odd-electron electronic configurations are obtained simply by adding or removing an electron, depending on the direction of the redox reaction, from each of the three closed-shell configurations *R*, *I*, and *P*. As we shall demonstrate, the mechanistic pathways and the reaction profiles for the electron transfer-assisted migratory insertion reactions are dictated by the energy needed to rearrange the key reacting electrons.

Oxidation-assisted migratory insertion. Catalytic oxidation of $cp(CO)_2Fe–CH_3$ (**5**) accelerates the rate of CO insertion by several orders of magnitude [20]. One explanation that has been forwarded asserts that the rate enhancement is due to reduced repulsion between the $Fe–CH_3$ bond pair and the Fe–CO bond pair in the oxidized species, $\{cp(CO)_2Fe–CH_3\}^+$ (**6**) [2b]. Other research, based on the investigation of ligand substitution reactions in 17-electron metal complexes, has suggested that oxidation of the starting metal alkyl complex, facilitates ligand assistance of the migration reaction [22].

The CM model provides a simple rationale for the catalytic effect of oxidation by considering the influence of oxidation on the relative energies of configurations *R*, *I*, and *P*. Removal of an electron from the starting material HOMO, a metal *d* orbital, decreases the extent of $d–\pi^*CO$ mixing. Hence, oxidation is expected to lower the energy of π^*_{MCO}, since π^*_{MCO} is formed by the destabilising interaction of d_M and π^*_{CO}. As a consequence, *I* and *P* will be stabilised relative to *R*, since *I* and *P* are generated from *R* by an electron shift into π^*_{MCO}. With *I* and *P* stabilized at the reactant geometry, a more rapid migration is predicted.

A second point of interest concerns the effect of oxidation on the degree of concertedness of the alkyl migration and the ligand (or solvent) attack at the metal. Does prior oxidation of the metal alkyl complex encourage a step-wise or a concerted process? As discussed previously, the answer depends on the relative energy of configuration *I* after oxidation. If oxidation leaves *I* relatively high in energy, then *I* will not contribute significantly to the wavefunction ($|c| < |a|$ and $|b|$, eq. 4), and a concerted, or ligand-assisted migration will result.

Oxidation, in fact, while stabilizing both *I* and *P*, affects the latter more, promoting a ligand-assisted reaction. The effect of oxidation on the relative energies of *I* and *P* is seen in its impact on the energies of σ_{MR} and σ_{ML}, both of which are lowered due to the increased electronegativity of the metal. Since *I* is generated from *R* by a $\sigma_{MR} \rightarrow \pi^*_{MCO}$ electron shift, the stabilization of *I* upon oxidation is rather small. *P*, on the other hand, can be obtained without ionizing the metal-centered orbitals by means of a $n_L \rightarrow \pi^*_{MCO}$ electron shift. Thus, oxidation stabilizes *P* to a significantly greater extent than *I*, leading to greater ligand assistance, as well as an enhanced reaction rate for the migration step [23*]. This predicted ligand-assistance has not been verified experimentally.

It has been suggested that oxidation of the metal alkyl complex might lead to metal–ligand bond formation, via a 3-electron interaction between n_L and d_M, prior to the actual migration step [22]. This mechanism may be difficult to distinguish from the concerted ligand-assisted migration pathway described above. Initial formation of a 3-electron M–L bond does not appear to affect the reacting electrons in a way that would accelerate the alkyl migration step, however, this kind of bonding might furnish a relatively low-energy pathway for the ligand to approach the metal center.

Reduction-assisted migratory insertion. Electrochemical reduction of $cp(CO)_2$-$Fe–CH_3$ (**5**) in the presence of PPh_3 results in the catalytic formation of $cp(CO)$-$(PPh_3)Fe–COCH_3$ [21]. The catalytic action of the added electron, as well as the isolation of a neutral 18-electron product, implies the generation of an odd-electron

* Reference number with asterisk indicates a note in the list of references.

intermediate that is capable of reducing **5**, and which can be converted to the acyl product. The mechanism that has been proposed [21] is shown in eqs. 13–16; the workers have associated the activation of the methyl complex with delivery of the odd electron into the Fe–CH_3 σ^* orbital [21]. The initial 19-electron complex, **7**, rearranges to give a 17-electron acyl complex, which is trapped by L, and which serves as a reducing agent, thereby sustaining the catalytic cycle.

$$\underset{(5)}{cp(CO)_2Fe\text{–}CH_3} + e^- \rightarrow \underset{(7)}{\{cp(CO)_2Fe\text{–}CH_3\}^-} \tag{13}$$

$$\underset{7}{\{cp(CO)_2Fe\text{–}CH_3\}^-} \rightarrow \{cp(CO)Fe\text{–}COCH_3\}^- \tag{14}$$

$$\{cp(CO)Fe\text{–}COCH_3\}^- + L \rightarrow \{cp(CO)LFe\text{–}COCH_3\}^- \tag{15}$$

$$\{cp(CO)LFe\text{–}COCH_3\}^- + \mathbf{5} \rightarrow cp(CO)LFe\text{–}COCH_3 + \mathbf{7} \tag{16}$$

The CM model for the reduction-assisted migration is based on three configurations R^-, I^-, and P^-, each of which is obtained by adding an electron to R, I, and P, respectively. Examination of each of the neutral configurations at their energy minima reveals that reduction stabilizes I relative to R and P. This stabilization of I is derived from the fact that the intermediate has a vacant, low energy, non-bonding orbital which can accept the added electron, whereas the acceptor orbitals for the reactant and product metal complexes are high energy antibonding orbitals.

If, as has been suggested for **5**, the added electron enters the σ^*_{MR} orbital of the metal alkyl complex, then the energy gap between R^- and I^- will also be reduced, relative to the R–I energy gap, at the *reactant* geometry. The $\sigma_{MR} \rightarrow \pi^*_{MCO}$ electron shift, which converts R into I, and R^- into I^-, requires less energy *after* reduction because it is easier to ionize a σ electron from an electron-rich 3-electron M–R bond

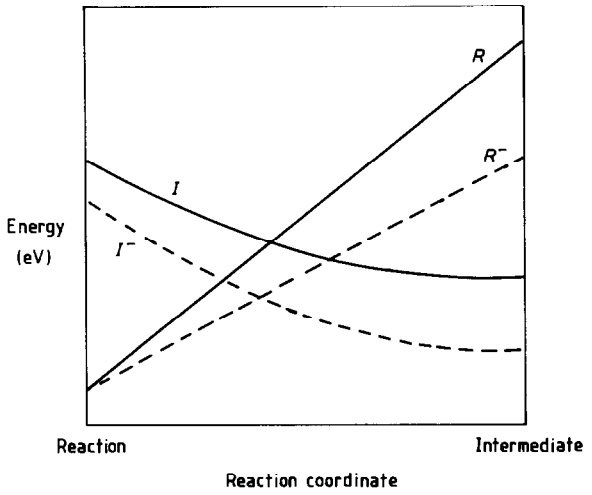

Fig. 6. Schematic energy diagram illustrating the effect of one-electron reduction on R and I (leading to configurations R^- and I^-). Dotted lines indicate a *lower* barrier for alkyl migration than for the unreduced complex.

than it is from a regular 2-electron σ bond. We also note that the energy of R^- does not rise as sharply during the migration as does the energy of R, since motion along the reaction coordinate for the reduced species involves stretching a weak 3-electron M–R bond.

The reaction profile for the reduction-assisted migration process is shown in Fig. 6. The profile is based on the three factors just discussed: the stabilization of I^- relative to R^- at the intermediate and reactant geometries, and the slow increase in energy of R^-. From the reaction profile it is obvious that we can expect reduction of the metal alkyl complex to accelerate the migratory insertion reaction via a step-wise process, i.e., migration of the alkyl group to give a relatively stable intermediate, followed by formation of the M–L bond.

Conclusion

This paper has attempted to demonstrate the utility of the CM model as applied to a classic organo-transition metal reaction. By considering the carbonyl insertion reaction in terms of VB and MO configurations, we have attempted to demonstrate that both the mechanistic spectrum and overall reactivity features may be appreciated in a simple qualitative way. This method of analysis does not require the construction of complex orbital correlation diagrams. Instead, identification of the two pairs of reacting electrons, and of the various electronic configurations produced by their reorganization, leads directly to the predictions made here.

As is true for essentially all organic reactions, the reaction profile may be built up from just three configurations, describing reactants, products, and a potential intermediate. Reactivity trends may be assessed by considering the effect of a given perturbation on the energy of I and P, while changes in the degree of concertedness of the reaction (step-wise or concerted) may be assessed by considering the effect of perturbations on the energy of I with respect to the R–P crossing point. Stabilization of I will encourage a step-wise precess.

A spectrum of mechanisms are predicted for migratory insertion reactions involving 18-electron metal alkyl carbonyl complexes. The nature of the migrating ligand, the migration terminus, the incoming ligand, and the solvent all play a role in determining the precise mechanism. Lewis acid catalysis is readily explained in terms of the effect of the acid on the $\pi^{\star}_{CO}$ orbital. Solvent-assisted migratory insertion can also be explained despite the apparent absence of a site for metal–solvent bond formation. Ligand, or solvent assistance, is also expected to characterize migratory insertions that are preceeded by oxidation of the starting metal alkyl complex. Initial reduction of the metal alkyl complex, on the other hand, will result in a stepwise migratory insertion. Regardless of the nature of the electron transfer, the CM model provides a simple explanation of the rate enhancements that have been reported.

No attempt has been made to explain every reactivity effect that has been observed in these systems. This goal is unrealistic given the qualitative nature of the CM model. Still, we have been able to describe the chemical reactivity trends for this basic reaction in a useful, but simple and straightforward manner. We believe that the CM model can be applied to other reactions of interest in organometallic chemistry, such as reductive elimination-oxidative addition reactions, and the reaction of metal-carbene complexes with alkenes.

Acknowledgement

A.P. thanks the Dept. of Chemistry, Stanford University for a visiting appointment during the tenure of which this manuscript was written. A.J.S. thanks the I.B.M. Research Division, San Jose, for a visiting appointment during the tenure of which part of this manuscript was written.

References

1 This reaction has been the subject of several reviews: (a) E.J. Kuhlmann and J.J. Alexander, Coord. Chem. Rev., 33 (1980) 195; (b) F. Calderazzo, Angew. Chem. Int. Ed. Engl., 16 (1977) 229; (c) A. Wojcicki, Adv. Organomet. Chem., 11 (1973) 85.
2 (a) H. Berke and R. Hoffmann, J. Amer. Chem. Soc., 100 (1978) 7224; (b) A. Cameron, V.H. Smith and M.C. Baird, Organometallics, 2 (1983) 465.
3 (a) D. Saddei, H.-J. Freund and G. Hohlneicher, J. Organomet. Chem., 186 (1980) 63; (b) M.E. Ruiz, A. Flores-Riveros and O. Novaro, J. Catal., 64 (1980) 1.
4 (a) A. Pross and S.S. Shaik, J. Amer. Chem. Soc., 104 (1982) 187; (b) S.S. Shaik and A. Pross, ibid., 104 (1982) 2708; (c) A. Pross and S.S. Shaik, Tetrahedron Lett., (1982) 5467; (d) A. Pross and S.S. Shaik, Acc. Chem. Res., 16 (1983) 363; (e) A. Pross, Adv. Phys. Org. Chem., 21 (1985) 99; (f) A. Pross, Acc. Chem. Res., 18 (1985) 212; (g) S.S. Shaik, Prog. Phys. Org. Chem., 15 (1985) 197; (h) T.H. Lowry and K.S. Richardson, Mechanism and Theory in Organic Chemistry, 3rd ed., Harper and Row, New York, 1987, pp. 219–222.
5 L. Pauling and E.B. Wilson, Jr. Introduction to Quantum Mechanics, McGraw-Hill, New York, 1935.
6 (a) K. Noack and F. Calderazzo, J. Organomet. Chem., 10 (1967) 101; (b) T.C. Flood, J.E. Jensen and J.A. Statler, J. Amer. Chem. Soc., 103 (1981) 4410.
7 (a) F. Calderazzo and F.A. Cotton, Inorg. Chem., 1 (1962) 30; (b) K. Noack, M. Ruch and F. Calderazzo, ibid., 7 (1968) 345; (c) R.J. Mawby, F. Basolo and R.G. Pearson, J. Amer. Chem. Soc., 86 (1964) 3994; (d) M. Green, R.I. Hancock and D.C. Wood, J. Chem. Soc. A, (1968) 2718; (e) B.L. Booth and E.J.R. Lewis, J. Chem. Soc., Dalton Trans., (1982) 417; (f) F. Calderazzo and K. Noack, Coord. Chem. Rev., 1 (1966) 118.
8 T.M. McHugh and A.J. Rest, J. Chem. Soc., Dalton Trans., (1980) 2323.
9 (a) S. Evans, J.C. Green, M.L.H. Green, A.F. Orchard and D.W. Turner, Discuss. Faraday Soc., 47 (1969) 112; (b) M.F. Guest, M.B. Hall and I.H. Hillier, Mol. Phys., 25 (1973) 629.
10 D.L. Lichtenberger and R.F. Fenske, Inorg. Chem., 13 (1974) 486.
11 F. Calderazzo and F.A. Cotton, Abstr. 7th Inter. Conf. Coord. Chem., Stockholm, 1962, Paper 6H7.
12 D.W. Kuty and J.J. Alexander, Inorg. Chem., 17 (1978) 1489.
13 (a) G.R. Dobson and E.P. Ross, Inorg. Chim. Acta, 5 (1971) 199; (b) H.C. Clark and T.L. Hauw, J. Organomet. Chem., 42 (1972) 429. The first carbonylation of a metal–silicon bond has been reported recently: T.D. Tilley, J. Amer. Chem. Soc., 107 (1985) 4084.
14 (a) S.B. Butts, S.H. Strauss, E.M. Holt, R.E. Stimson, N.W. Alcock and D.F. Shriver, J. Amer. Chem. Soc., 102 (1980) 5093; (b) S.B. Butts, T.G. Richmond and D.F. Shriver, Inorg. Chem., 20 (1981) 278; (c) T.G. Richmond, F. Basolo, D.F. Shriver, Inorg. Chem., 21 (1982) 1272; (d) J.P. Collman, R.G. Finke, J.N. Cawse and J.I. Brauman, J. Amer. Chem. Soc., 100 (1978) 4766; (e) J.A. Labinger, J.N. Bonfiglio, D.L. Grimmett, S.T. Masuo, E. Shearin and J.S. Miller, Organometallics, 2 (1983) 733; (f) T.C. Forschner and A.R. Cutler, Organometallics, 4 (1985) 1247.
15 (a) W.P. Weiner and R.G. Bergman, J. Amer. Chem. Soc., 105 (1983) 3922; (b) M.D. Seidler and R.G. Bergman, Organometallics, 2 (1983) 1897.
16 E. Singleton and H.E. Oosthuizen, Adv. Organomet. Chem., 22 (1983) 209.
17 J.D. Cotton and G.T. Crisp and L. Latif, Inorg. Chim. Acta, 47 (1981) 171.
18 (a) M.J. Wax and R.G. Bergman, J. Amer. Chem. Soc., 103 (1981) 7028; (b) J.C. Cotton and R.D. Markwell, Organometallics, 4 (1985) 937.
19 A review of the EHMO calculation reported in ref. 2a arrived at the conclusion that the transition state for alkyl migration is dominated by the mixing of the σ_{MR} and π^*_{MCO} orbitals: T.A. Albright, Tetrahedron, 38 (1982) 1339. An ab-initio investigation of alkyl migrations in Pd complexes has also reached the same conclusion: N. Koga and K. Morokuma, J. Amer. Chem. Soc., 107 (1985) 7230.

20 R.H. Magnuson, S.J. Zulu, W.-M. T'sai and W.P. Giering, J. Amer. Chem. Soc., 102 (1980) 6887. R.H. Magnuson, R. Meirowitz, S.J. Zulu and W.P. Giering, ibid., 104 (1982) 5790. R.H. Magnuson, R. Meirowitz, S.J. Zulu and W.P. Giering, Organometallics, 2 (1983) 460. D.L. Reger and E. Mintz, Organometallics, 3 (1984) 1759.
21 D. Miholova and A.A. Vlcek, J. Organomet. Chem., 240 (1982) 413.
22 K.M. Doxsee, R.H. Grubbs and F.C. Anson, J. Amer. Chem. Soc., 106 (1984) 7819.
23 A 15-electron metal acyl complex, such as $\{cp(CO)Fe\text{–}COCH_3\}^+$, should be more unstable and more reactive towards an incoming ligand than its 16-electron analog. This is consistent with the stabilization of *P* relative to *I* after oxidation.